

Predicting trends in atmospheric CO₂ across the Mid-Pleistocene Transition using existing climate archives

Jordan R.W. Martin¹, Joel Pedro^{2,3}, Tessa R. Vance³

¹Institute for Marine and Antarctic Studies, University of Tasmania, Hobart, 7004, Australia

²Australian Antarctic Division, Kingston, 7050, Australia

³Australian Antarctic Program Partnership, Institute for Marine and Antarctic Studies, University of Tasmania, Hobart, 7004, Australia

Correspondence to: Jordan R.W. Martin (jrmartin@utas.edu.au)

Abstract

During the Mid-Pleistocene Transition (MPT), ca. 1200–800 thousand years ago (kya), the Earth's glacial cycles changed from 41 kyr to 100 kyr periodicity. The emergence of this longer ice-age periodicity was accompanied by higher global ice volume in glacial periods and lower global ice volume in interglacial periods. Since there is no known change in external orbital forcing across the MPT, it is generally agreed that the cause of this transition is internal to the earth system. Resolving the climate, carbon cycle and cryosphere processes responsible for the MPT remains a major challenge in earth and palaeoclimate science. To address this challenge, the international ice core community has prioritised recovery of an ice core record spanning the MPT interval.

Here we present results from a simple generalised least squares (GLS) model that predicts atmospheric CO₂ out to 1.8 Myr. Our prediction utilises existing records of atmospheric carbon dioxide (CO₂) from Antarctic ice cores spanning the past 800 kyr along with the existing LR04 benthic $\delta^{18}\text{O}_{\text{calcite}}$ stack (Lisiecki & Raymo, 2005; hereafter 'benthic $\delta^{18}\text{O}$ stack') from marine sediment cores. Our predictions assume that the relationship between CO₂ and benthic $\delta^{18}\text{O}$ over the past 800 thousand years can be extended over the last one and a half million years. The implicit null hypothesis is that there has been no fundamental change in feedbacks between atmospheric CO₂ and the climate parameters represented by benthic $\delta^{18}\text{O}$, global ice volume and ocean temperature.

We test the GLS-model predicted CO₂ concentrations against observed blue ice CO₂ concentrations, $\delta^{11}\text{B}$ -based CO₂ reconstructions from marine sediment cores and $\delta^{13}\text{C}$ of leaf-wax based CO₂ reconstructions (Higgins *et al.*, Yan *et al.*, 2019 and Yamamoto *et al.*, 2022). We show that there is not clear evidence from the existing blue ice or proxy CO₂ data to reject our predictions nor our associated null-hypothesis. A definitive test and/or rejection of the null hypothesis may be provided following recovery and analysis of continuous oldest ice core records from Antarctica, which are still several years away. The record presented here should provide a useful comparison for the oldest ice core records and opportunity to provide further constraints on the processes involved in the MPT.

37 **1 Introduction**

38 Ice core records from Antarctica provide comprehensive and continuous records of many climate parameters
39 over the last 800 thousand years, e.g. from the Vostok (Petit *et al.*, 1999) and European Project for Ice Coring in
40 Antarctica's Dome-C (EDC) ice cores (Jouzel *et al.*, 2007). One of the major challenges in climate science lies
41 beyond the current threshold of the ice core record. The Mid-Pleistocene Transition (MPT) spans from ca.
42 1200–800 thousand years ago (kya) (Chalk *et al.*, 2017) and is characterised by a change from regularly paced
43 40 thousand year (kyr) glacial cycles with thinner glacial ice sheets to quasi-periodic 100 kyr glacial cycles in
44 which ice sheets are more persistent and thicker (Clark *et al.*, 2006, Chalk *et al.*, 2017). To resolve the forcings
45 and feedbacks involved in this transition, multiple nations are targeting recovery of continuous ice cores
46 spanning the MPT under the framework of the International Partnerships in Ice Core Science (IPICS) oldest ice
47 core challenge (IPICS, 2020).

48

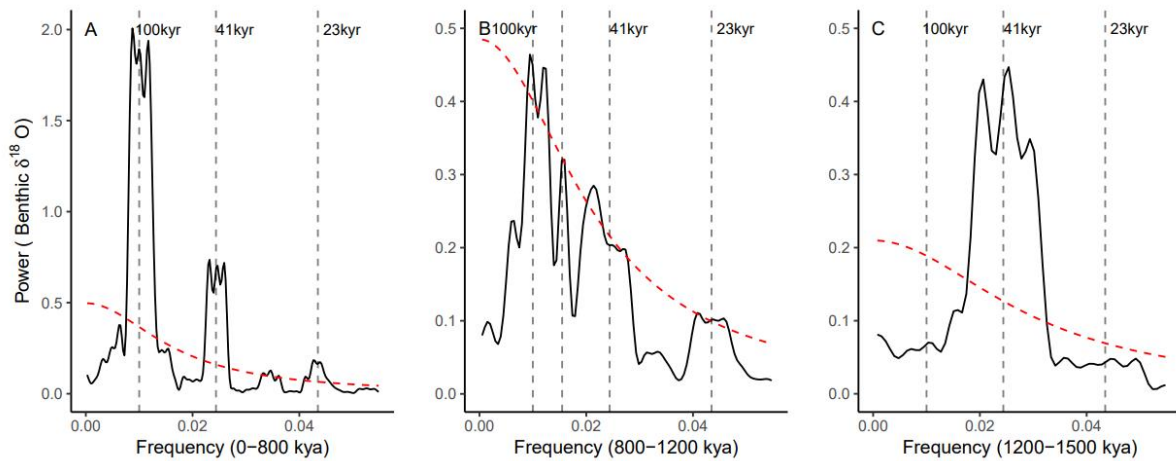
49 The purpose of the current study is to make a simple prediction of atmospheric CO₂ across the MPT. Cross-
50 comparison of our and other predicted CO₂ records against observed MPT CO₂ data will aid in testing
51 competing hypotheses on the cause of the transition, in particular the role of carbon cycle changes.

52

53 The MPT occurred in the absence of any changes to orbital insolation forcing; therefore, the mechanisms behind
54 the MPT must be internal to the earth system (Raymo, 1997; Ruddiman *et al.*, 1989). Multiple hypotheses have
55 been put forward to explain the transition. A common element in many of these is internal climate/earth system
56 changes which allow for the development of thicker, more extensive ice sheets that could endure insolation
57 peaks corresponding to the 23 kyr precession and 41 kyr obliquity cycles, i.e., an increase in the threshold for
58 deglaciation and altered sensitivity to orbital forcings (McClymont *et al.*, 2013; Tzedakis *et al.*, 2017). Indeed,
59 the skipped obliquity cycle hypothesis, proposes that 100 kyr signal seen in spectral analysis of the post-MPT
60 benthic $\delta^{18}\text{O}$ stack (e.g. Fig 1A) may be comprised of alternating 80 and 120-kyr signals, i.e. in which the
61 intervening obliquity cycles are skipped. Among the prominent hypotheses to explain an increased threshold for
62 deglaciation are the following three.

- 63 1) A long- term decrease in radiative forcing due to a secular reduction in atmospheric CO₂ across the
64 transition (e.g. Berger *et al.*, Hönisch *et al.*, 2009; 1999, Raymo *et al.*, 1988). According to this view,
65 reduced radiative forcing drives the formation of larger and more stable ice sheets.
- 66 2) Progressive removal of sub-glacial regolith during the 41 kyr glacial cycles. Clark & Pollard (1998)
67 proposed that ice sheet basal sliding prior to the MPT was enhanced by the presence of a low-friction
68 sedimentary regolith layer between the Laurentide ice sheet and the crystalline bedrock. According to
69 this view, progressive removal of this sedimentary layer then favoured the development of larger and
70 more persistent post-MPT ice sheets.
- 71 3) Phase-locking of the Northern and Southern Hemisphere ice sheets. In frequency spectra of the global
72 marine benthic $\delta^{18}\text{O}$ record (Fig. 1) there is no evidence of the precession (23 kyr) component of
73 northern hemisphere insolation prior to the MPT; the spectra is dominated by the obliquity (41 kyr)
74 component (Fig. 1C). Emergence of significant precession and 100 kyr signals occurs across the MPT
75 (Fig. 1B), and all three components are clearly present after the MPT (Fig. 1A). Raymo *et al.* (2006)
76 suggested that precession-paced changes in northern and southern hemisphere ice volumes may have

77 occurred prior to the MPT, but are cancelled due to out-of-phase ice volume changes between the two
 78 hemispheres. According to this view, during the MPT the precession-paced changes fall into phase
 79 between the two hemispheres, such that the precession signal emerges (Raymo *et al.*, 2006). In this
 80 view the global synchronisation of ice volume drives the formation of larger and more stable ice sheets.
 81
 82 These hypotheses are not mutually exclusive. For a recent review on the cause of the MPT see Berends *et al.*
 83 (2021a).
 84



85
 86
 87 **Figure 1: Thomson Multi-taper Method (MTM) spectral analysis representing relative power of signal periodicity for:**
 88 **A) Benthic $\delta^{18}\text{O}$ stack after (0–800 kya) the Mid-Pleistocene Transition (MPT); B) Benthic $\delta^{18}\text{O}$ across the MPT (800–**
 89 **1200 kya); C) Benthic $\delta^{18}\text{O}$ prior to the onset of the MPT (1200 kya–1500 kya). Each with a robust AR (1) 95 %**
 90 **Confidence interval (red dashed line). Benthic $\delta^{18}\text{O}$ stack data from Lisiecki and Raymo (2005).**
 91

92 For a long-term decrease in radiative forcing by atmospheric CO_2 to be the cause of the MPT, the reduction in
 93 CO_2 might be expected in both glacial and interglacial stages (Chalk *et al.*, 2017). However, low resolution
 94 boron-isotope-based CO_2 reconstructions by Hönisch *et al.*, (2009), and Chalk *et al.*, (2017) suggest that glacial-
 95 stage CO_2 drawdown occurred over the MPT in the absence of interglacial CO_2 drawdown. Glacial-stage CO_2
 96 draw-down across the MPT may be a positive climate-carbon cycle feedback to changes in ice sheet dynamics,
 97 including CO_2 drawdown by enhanced iron fertilisation of the Southern Ocean in response to exposed
 98 continental shelves due to lower sea level, as well as planetary drying associated with colder climate conditions
 99 (Chalk *et al.*, 2017). Colder glacial temperatures that enhance the solubility of CO_2 in the oceans, and reduced
 100 abyssal ocean ventilation has also been implicated in enhanced glacial-stage ocean storage of CO_2 (McClymont
 101 *et al.*, 2013; Hasenfratz *et al.*, 2019).
 102

103 Testing of hypotheses on the cause of the MPT is currently limited by the lack of a continuous ice core that
 104 spans its duration. The International Partnership in Ice Core Sciences (IPICS) has nominated recovery of such a
 105 record as a key priority in ice core research (IPICS, 2020). Multiple national and international projects have
 106 commenced, or are soon to commence, drilling for ‘oldest ice’ (see e.g. Shugi, 2022). In this project, we take
 107 inspiration from the “EPICA Challenge” in which the paleoclimate and modeling community was challenged to

108 predict the global atmospheric carbon dioxide and methane concentrations from 800–400 kya based on the
109 existing 400 kyr Vostok ice core record (Wolff *et al.*, 2004). Here, we use a generalised least squares (GLS)
110 model trained on continuous climate archives to predict a CO₂ record out 1.8 Mya. We utilise two primary data
111 sets for the GLS model: the existing 800 kyr ice core composite record of atmospheric CO₂ (Bereiter *et al.*,
112 2015) and the LR04 benthic stack of 57 globally-distributed records of the ¹⁸O to ¹⁶O ratio of fossil benthic
113 foraminifera calcite (hereafter referred to as the LR04 $\delta^{18}\text{O}$ benthic stack). The $\delta^{18}\text{O}$ ratios in the LR04 benthic
114 stack are governed primarily by deep ocean temperature and global ice volume at the time the foraminifera
115 lived, with higher values indicating both increased ice volume and a colder climate. The relationship between
116 the ice volume and ocean temperature components contributing to the $\delta^{18}\text{O}$ benthic stack are not linear.
117 Separating the two signals remains challenging and has been attempted elsewhere using a range of approaches
118 from comparison with paired deep ocean temperature proxies (Elderfield *et al.*, 2012), inverse modelling
119 (Berends *et al.*, 2021b) and spectral analysis (e.g. Huybers and Wunsch, 2009).

120

121 Fig. 2 shows a scatter-plot of the LR04 $\delta^{18}\text{O}$ benthic stack versus observed ice core CO₂ over the past 800 kyr.
122 Both data sets are binned to equivalent 3-kyr time steps (Methods). The Pearson's correlation coefficient (*r*)
123 between the data sets is -0.82 (*p* < 0.05) indicating that ~68% of the variance in observed CO₂ is shared with the
124 LR04 $\delta^{18}\text{O}$ benthic stack. This strong relationship provides an initial rationale for using the LR04 $\delta^{18}\text{O}$ benthic
125 stack as an input parameter to predict CO₂ beyond 800 kyr. Mechanistically, multiple processes are expected to
126 contribute to the shared variance. A first order factor is the dependency of CO₂ solubility on ocean temperature
127 (e.g. Millero, 1995). From the simple solubility perspective, colder climate states with increased ice volume and
128 colder ocean temperatures will drive increased ocean uptake of CO₂ (Berends *et al.*, 2021a). However, the
129 solubility effect only accounts for a portion of observed glacial CO₂ drawdown (Archer *et al.*, 2000). Multiple
130 additional contributors to the shared variance are proposed in the literature. These include (not exhaustively),
131 direct radiative forcing of ice volume changes by CO₂ (e.g. Shackleton *et al.*, 1985); the impact of ice
132 volume/sea level changes on atmospheric CO₂ via ocean productivity and carbonate chemistry changes (e.g.
133 Broecker, 1982; Archer *et al.*, 2000; Ushie and Matsumoto, 2012); CO₂ drawdown during periods of high ice
134 volume by increased iron fertilisation (e.g. Röthlisberger *et al.*, 2004; Martinez-Garcia *et al.*, 2014) and
135 enhanced sea ice extent during periods of high ice volume capping the ventilation of CO₂ from the ocean
136 interior at high latitudes (Stephens and Keeling, 2000).

137

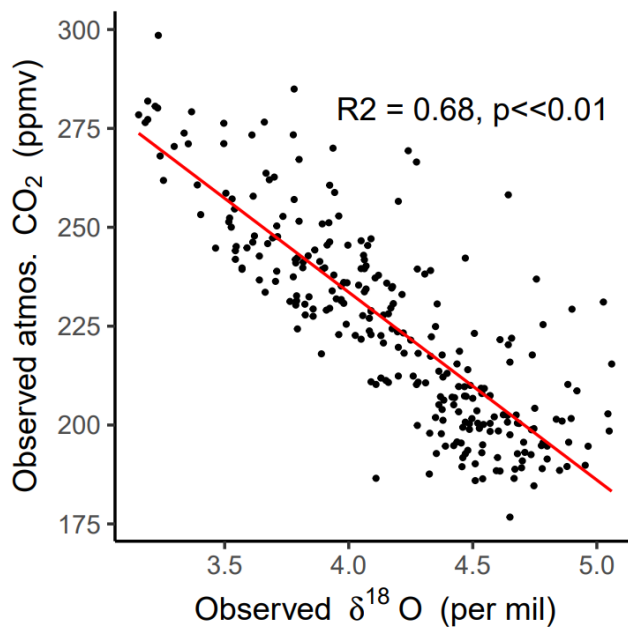
138 A quantitative separation and attribution of the processes linking global ice volume, ocean temperature and
139 atmospheric CO₂ on millennial to orbital timescales is not currently available (e.g. Archer *et al.*, 2000; Sigman
140 *et al.*, 2010; Gottschalk *et al.*, 2019) and will not be attempted here. Rather, we make the simple assumption that
141 the relationships between the LR04 benthic $\delta^{18}\text{O}$ stack and CO₂ can be extended beyond 800 kya and use
142 generalised least squares (GLS) regression modelling between benthic $\delta^{18}\text{O}$ and CO₂ to make a prediction of
143 CO₂ spanning 800–1500 kya. The deliberately simple implicit assumption, and null hypothesis, is that there is
144 no change to the feedback processes linking benthic $\delta^{18}\text{O}$ and CO₂ before and after the MPT.

145

146 This approach differs to previous more complex model studies that have attempted to reconstruct CO₂ using the
147 LR04 benthic $\delta^{18}\text{O}$ stack as an input variable (van de Wal, 2011; Stap *et al.*, 2016, Berends *et al.*, 2021b). The

148 latter studies use an inverse forward modelling approach, in which climate and ice sheet models of various
 149 complexities are used to capture physical relations between CO₂, global temperature and ice volume. For
 150 example, in Berends *et al.*, 2021b the offset between modelled and observed benthic δ¹⁸O is used to calculate a
 151 value for atmospheric CO₂ that is iterated back to the inverse model. The CO₂ record which minimises the
 152 difference between the modelled and observed benthic stack is then taken as an estimate of how atmospheric
 153 CO₂ may have evolved to force coupled climate, deep ocean temperature and land ice volume changes that
 154 reproduce the observed benthic δ¹⁸O signal. Accuracy of the reconstructions in the inverse modelling approach
 155 depends on the ability of the climate and ice sheet models used to capture the correct climate dynamics across
 156 the MPT. Our GLS method is a simpler statistical approach, designed with the specific null hypothesis in mind,
 157 that does not attempt to simulate the physics linking benthic δ¹⁸O signal, land ice volume, global temperature
 158 and CO₂. A range of approaches to reconstructing CO₂ have been called for and are of value in the context of
 159 forthcoming continuous ice core records across the MPT from oldest ice projects currently underway in
 160 Antarctica [IPICS 2020].

161



162 **Figure 2: Scatter plot of the composite observed atmospheric CO₂ record (Bereiter *et al.*, 2015) against**
 163 **the LR04 benthic stack of marine δ¹⁸O records (Lisiecki & Raymo, 2005). Red line is a linear line of best**
 164 **fit ($R^2 = 0.68$; $p < 0.05$).**

165

166 To test our null hypothesis, in advance of the recovery of a continuous ice core, we compare our predicted CO₂
 167 record to two sets of low-resolution ice core data that exist outside the current 800 kyr observed CO₂. These data
 168 come from direct CO₂ measurements from ancient “blue ice” from the Allan Hills in East Antarctica (hereafter
 169 referred to as BI-CO₂) from ca. 1 Mya (Higgins *et al.*, 2015) and 1.5 Mya (Yan *et al.*, 2022). We use the term
 170 blue ice to describe deep, ancient glacial ice that has been brought nearer to the surface of an ice sheet by ice
 171 flow. Blue ice is sampled by cutting trenches or shallow drilling of up to several hundred meters (e.g. Higgins *et*
 172 *al.*, 2015). The vertical migration of blue ice is associated with high deformation making the ice samples
 173 stratigraphically complex and hard to date (Higgins *et al.*, 2015). As a result, blue ice records alone do not

174 provide a continuous CO₂ record across the MPT. In the Discussion, we also compare our predicted record to
175 existing proxy-CO₂ reconstructions from boron-isotope analysis of benthic foraminifera in marine sediment
176 records (Chalk, *et al.*, 2017; Dyez *et al.*, 2018; Guillermic *et al.*, 2022), leaf wax δ¹³C carbon isotope ratios
177 (Yamamoto *et al.*, 2022) and predictions from previous models of various complexities (van de Wal *et al.*, 2011;
178 Willeit *et al.* 2019; Berends *et al.* 2021b). We conclude with discussion of the implications of our results and
179 data-comparisons for the understanding MPT dynamics.

180

181 **2 Methods**

182

183 We use a generalised least squares (GLS) model with an auto-regressive (AR) factor 1 to predict atmospheric CO₂
184 from the LR04 benthic δ¹⁸O stack (Fig. 3A and B). We use GLS because the assumptions of ordinary least squares
185 (OLS) are violated by the presence of autocorrelation and heteroskedasticity in the regression errors. We selected
186 the AR(1) correlation factor as it yielded the lowest Akaike information criterion (AIC) value from a test of
187 multiple correlation factors. The AR(1) process assumes and accounts for dependence of error at a given point in
188 time on the previous error term. In practise this makes the model assumptions more realistic and improves
189 parameter estimation where, as in the climate system, observations are dependent on past values.

190

191 To obtain common time steps and resolution between the predictor (LR04 benthic δ¹⁸O stack) and response
192 (CO₂) variables, we re-grid the LR04 benthic stack and Bereiter *et al.*, (2015) CO₂ data into time bins with a
193 resolution of 3-kyr. The GLS regression model was then applied over the 0 – 800 kyr range of the predictor and
194 response variables as follows:

195

$$196 \quad CO_2 = -33.37 \times \delta^{18}O + 365.15, \text{ autoregressive (AR) factor: } 1$$

197

198 Based on the regression model, the δ¹⁸O values of the LR04 Benthic Stack from 800 – 1500 kya were used to
199 predict CO₂ concentration over this range (hereafter referred to as PRED-CO₂). To gauge the GLS model
200 stability we took a bootstrap approach, selecting a random 50% subset of our data (with replacement) and re-
201 running the model 1000 times to determine 95% confidence intervals for the predictions. While the GLS method
202 itself addresses autocorrelation, the bootstrap method introduces variability such that each iteration of the model
203 has different combinations of the original data points (including repeated ones), this variability helps in
204 assessing the robustness and sensitivity of the model e.g. to variable data and dating uncertainty.

205

206 Uncertainties in the independent age scales of both the LR04 stack and the compiled CO₂ record are inherited by
207 our GLS model and its predictions. The LR04 stack includes 57 globally-distributed benthic δ¹⁸O sediment core
208 records. The age models for these cores are constructed by alignment of their δ¹⁸O signals, followed by tuning
209 of the stack to a simple ice model based on 21 June insolation at 65°N in a way which maintains relatively
210 stable global mean sedimentation rates. (Lisiecki & Raymo, 2005). The authors estimate uncertainty of 6 kyr
211 from 1.5 – 1.0 Mya and 4 kyr from 1 – 0 Mya (Lisiecki & Raymo, 2005). The observed CO₂ composite ice core
212 record for the past 800 kya (Bereiter *et al.*, 2015) uses six independent dating methods for various core locations
213 both spatially across Antarctica, and stratigraphically for different sections of the same core. The age uncertainty
214 in the gas timescale has a median over the 0 – 800 kya interval of 2 kyr, but individual uncertainties can reach

215 up to 5 kyr (Veres *et al* 2013; Bazin *et al.*, 2013). The relative age uncertainties between these input variables
216 may diminish the regression or in some instances lead to spurious correlation. However, we expect any such
217 effects are minor on the basis that our predictions show little sensitivity to the bootstrap analysis; with a median
218 2σ error of 5.8 ppm from 0 to 1.8 Mya (see Fig. 3B, C and Discussion).

219

220 **3 Results**

221 Fig. 3B shows the time series of our LR04 benthic $\delta^{18}\text{O}$ stack-based GLS model predictions of atmospheric CO_2
222 (PRED- CO_2) over the past 800 kyr, in comparison to the observed ice core CO_2 record from Bereiter *et al.*,
223 (2015). The correlation coefficient (R^2) between the predicted and observed records is 0.68 ($p \ll 0.01$). Our
224 PRED- CO_2 record out to 1.8 Mya with shaded 95% CIs from the bootstrap analysis is also shown, overlain with
225 observed Allan Hills blue ice CO_2 (BI- CO_2) datasets of age 1000 ± 89 kya (Higgins *et al.*, 2015) and $1.5 \text{ Mya} \pm$
226 213 kyr (Yan *et al.*, 2022).

227

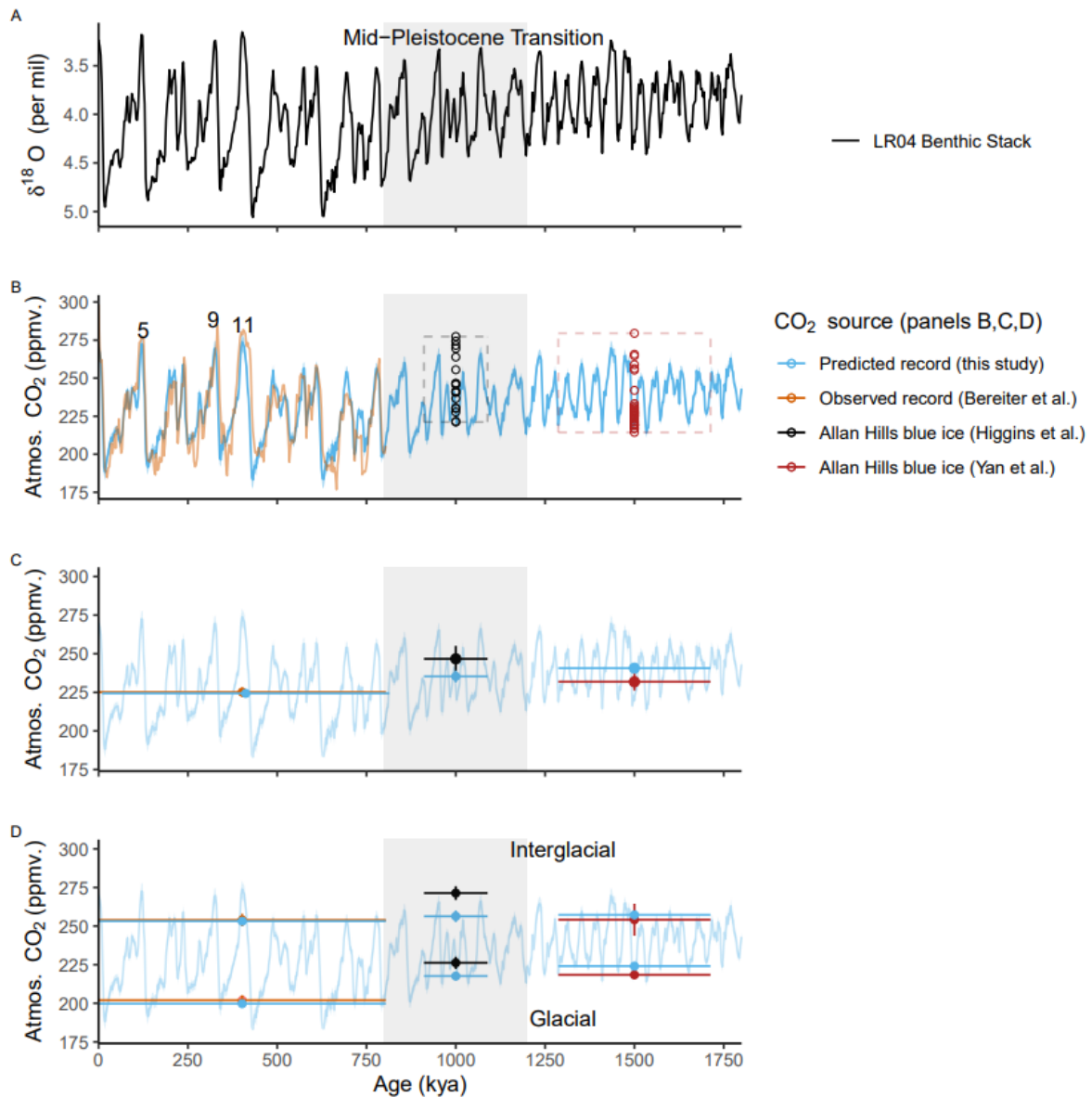
228 We evaluate the PRED- CO_2 record against the observed CO_2 data according to criteria of mean concentrations
229 across the common intervals, and mean concentrations in the glacial and interglacial subsets of the data. First,
230 the mean CO_2 concentration over the common intervals (Fig 3C). From 0 – 800 kya the mean concentration in
231 observed (Bereiter *et al.*, 2015) and PRED- CO_2 data are in close agreement (225.2 ± 3.03 ppm versus the
232 predicted 225.2 ± 2.5 ppm respectively; uncertainties are 95% confidence intervals, i.e. 1.96σ). In the 1000 ± 89
233 kya interval (i.e. averaged across the age uncertainty of the Higgins *et al.* (2015) blue ice data) the BI- CO_2
234 concentration is ~ 11 ppm higher than PRED- CO_2 (246.7 ± 8.4 ppm versus the predicted 235.3 ± 3.9 ppm), this
235 difference is not significant at the 95% confidence level. For the $1.5 \text{ Mya} \pm 213$ kyr interval, the mean BI- CO_2
236 concentration is ~ 9 ppm lower than PRED- CO_2 (231.9 ± 5.6 ppm versus the predicted 240.7 ± 2.1 ppm), which
237 is marginally significant at the 95% level. Comparisons of mean levels across intervals spanning multiple glacial
238 and interglacial cycles may be biased if (as is likely) the blue ice data is not sampling glacial and interglacial
239 values with the same uniformity as a continuous record.

240

241 To address this, we define the glacial and interglacial thresholds of PRED- CO_2 to be respectively the lower and
242 upper 25th percentiles of the LR04 $\delta^{18}\text{O}$ predictor variable (following Chalk *et al.*, 2017). Filtering the observed
243 (Bereiter *et al.*, 2015) CO_2 record and our predicted CO_2 record according to these definitions we find a very
244 close match for glacial (202.0 ± 3.2 versus the predicted 199.7 ± 1.6 ppm) and interglacial intervals (253.9 ± 4.1
245 ppm versus the predicted 253.1 ± 2.3 ppm), over the past 800 kya (see Fig. 3D for these comparisons). For blue
246 ice (BI- CO_2) data, a corresponding LR04 isotope signal could not be confidently applied to the measured CO_2
247 concentration due to the uncertainties associated with blue ice dating; therefore, we defined the glacial and
248 interglacial thresholds of blue ice data according to the top (interglacial) and bottom (glacial) 25th percentiles of
249 actual CO_2 . Applying this to the 1000 ± 89 kya interval finds that observed BI- CO_2 data is ~ 9 ppm higher than
250 PRED- CO_2 during the glacial stages (226.2 ± 4.0 ppm versus the predicted 217.6 ± 2.3 ppm) and ~ 15 ppm
251 higher than PRED- CO_2 during the interglacial stages (271.3 ± 4.5 versus the predicted 256.3 ± 3.8 ppm). These
252 differences are significant with respect to the constrained uncertainties. During the $1.5 \text{ Mya} \pm 213$ kyr interval,
253 the mean BI- CO_2 concentration did not show any significant difference to PRED- CO_2 in interglacial stages
254 (254.1 ± 10.3 versus the predicted 257.2 ± 1.7 ppm. During glacial stages there is a small 2.9 ppm difference

255 between the upper estimate of BI-CO₂ and the lower estimate of PRED-CO₂ (218.4 ± 1.3 and 224 ± 1.4 ppm
 256 respectively, see Fig 3D). In our view these results, notwithstanding the 2.9 ppm difference at 1.5 Mya, do not
 257 give sufficient cause to reject the GLS model. Furthermore, the comparison indicates that PRED-CO₂ is not
 258 drifting systematically away from the existing observed BI-CO₂ data (Fig 3D). The differences could of course
 259 be a failing in the model, potential biases in the blue ice data, dating uncertainty and/or other unconstrained
 260 uncertainties (see Discussion for blue ice caveats).

261



262
 263 **Figure 3: A) The LR04 Benthic Stack of 57 globally distributed δ¹⁸O records (Lisiecki & Raymo, 2005).**
 264 **B) Comparison of our PRED-CO₂ (ppm) record to the current continuous composite record (0–800 kya);**
 265 **and to direct CO₂ measurements from Allan Hills blue ice cores (BI-CO₂) ca. 1 Mya (± 89 kyr) (Higgins *et***
 266 ***al.*, 2015) and ca. 1.5 Mya (± 213 kyr) (Yan *et al.*, 2022). Age uncertainty boundaries for the BI-CO₂ data**
 267 **are represented by dashed box boundaries. Marine isotope stages 5, 9, and 11 are numbered on the plot**
 268 **according to Lisiecki & Raymo (2005). Blue shading around PRED-CO₂ is the 95% CI from bootstrap**
 269 **analysis. C) Mean concentrations of the PRED-CO₂ and observed composite CO₂ records over the range**

270 **of the observed composite record (offset for clarity), and the mean concentrations of the PRED-CO₂ and**
271 **BI-CO₂ data at 1 Mya and again at 1.5 Mya averaged over the age uncertainty range of each BI-CO₂ data**
272 **set. D) As for C) however filtered by the upper and lower 25th and 75th percentiles to estimate glacial and**
273 **interglacial periods.**

274

275 We now consider long-term trends in interglacial and (separately) glacial CO₂ levels across the past 1.8 Myr in
276 PRED-CO₂ and in the existing ice core CO₂ data. For PRED-CO₂ there is no significant difference between CO₂
277 concentrations in the interglacial stages of the 1.5 Mya ± 213 kya, 1000 ± 89 kya and 0–800 kya windows (Fig 4
278 D, blue bars). In the ice core observations, interglacial levels at 1.5 Mya in BI-CO₂ are also within the
279 uncertainties of those in the 0–800 kya interval. Notably, the BI-CO₂ concentrations in the 1000 ± 89 kya
280 interval appear elevated with respect to the 0–800 kyr and 1.5 Mya ± 213 kya intervals, however this elevated
281 (ca. 271 ppm) level is consistent with the observed interglacial CO₂ concentration during interglacials 5, 9 and
282 11 (Fig 3B). Overall, there is no indication in the observed ice core CO₂ data or in PRED-CO₂ for a long-term
283 trend in *interglacial* CO₂ levels across the past 1.8 Myr.

284

285 In comparison, there are significant declines in glacial CO₂ levels across the MPT in PRED-CO₂ and the
286 observed ice core data. For PRED-CO₂, glacial CO₂ concentrations are not significantly different during the 1.5
287 Mya ± 213 kya and 1000 ± 89 kya windows. However, across the MPT, PRED-CO₂ glacial concentrations drop
288 by ~18 ppm (Fig 3D). This pattern is similar to the observed BI-CO₂ data, where glacial CO₂ levels show no
289 decline between the 1.5 Mya ± 213 kya and 1000 ± 89 kya windows (indeed there is a marginal increase from
290 218.4 ± 1.3 to 226.2 ± 4.0 ppm, respectively), before falling by 24 ppm to the 0–800 kyr observed glacial mean
291 of 202.0 ± 3.2 ppm (Fig 3D). Glacial-stage draw-down of CO₂ across the MPT in the absence of interglacial
292 draw-down is consistent with previous observations based on the boron-isotope-based CO₂ reconstructions (e.g.,
293 Chalk *et al.*, 2017; Hönlisch *et al.*, 2009 and see Discussion). In the following section we also compare PRED-
294 CO₂ data to boron-isotope-based and other CO₂ proxy records covering the 0 to 1.8 Myr interval.

295

296 **4 Discussion**

297 Our objective with this manuscript was to generate the simplest reasonable model to predict CO₂ from the LR04
298 δ¹⁸O benthic stack and to test the predictions against available observations. It is possible that the fit between
299 observed and our predicted CO₂ data could be further improved using a non-linear approach. However, we
300 refrain from a non-linear approach for several key reasons. First, a scatter plot of the LR04 δ¹⁸O benthic stack
301 versus observed ice core CO₂ over the past 800 kyr yields a Pearson's correlation coefficient (R) of -0.82 (Fig.
302 2), indicating that ~68% of the variance in observed CO₂ is shared with the benthic stack. This is similar to that
303 reported in ordinary linear least-squares regression (R²=0.70) by Berends *et al.* (2021b). Importantly, there is no
304 evidence in this scatter plot for departure from the linear relationship at high or low CO₂ or benthic δ¹⁸O levels.
305 Second, following the approach of Chalk *et al.*, 2017 and interpreting the upper 25th percentile of CO₂ data as
306 representing mean interglacial stage CO₂ and the lower 25th percentile of CO₂ data as representing mean glacial
307 stages CO₂ levels, we see that our predicted interglacial mean value for the past 800 kyr (253.1 ± 2.3 ppm)
308 closely overlaps with the observed interglacial mean value (253.9 ± 4.1 ppm) and similarly, the predicted glacial
309 stage mean (199.7 ± 1.7 ppm) closely overlaps with the observed glacial stage mean (202.0 ± 3.2 ppm). Third,

310 the predictions are remarkably insensitive to bootstrap analysis in which 50 % of that data are omitted with each
311 iteration of the GLS model. Such insensitivity to the bootstrap analysis and accurate prediction of glacial and
312 interglacial state CO₂ values would be unlikely in the case of major non-linear dependencies between the LR04
313 predictor and CO₂ response variables. Fourth, non-linear approaches would risk generating an improved fit due
314 to statistical artefacts that do not meaningfully relate to any dependence between benthic δ¹⁸O and CO₂. Finally,
315 the specific causes and sources and sinks involved in glacial to interglacial and millennial-scale CO₂ variations
316 remain poorly constrained (e.g. Archer *et al.*, 2000; Sigman *et al.*, 2010; Gottschalk *et al.*, 2019). Given this
317 process-uncertainty, the GLS model fits our criteria of the simplest reasonable model. Further, the use of benthic
318 δ¹⁸O to predict atmospheric CO₂ has precedence; in response to the EPICA challenge (Wolff *et al.*, 2004) N.
319 Shackleton predicted atmospheric CO₂ out to 800 kyr, based on a number of benthic δ¹⁸O records from the East
320 Pacific (Wolff, 2005).

321

322 There are several caveats with blue ice data that may affect its use to evaluate our GLS model predictions. The
323 blue ice data may have been subject to diffusional smoothing of CO₂ (e.g. Yan *et al.*, 2019), which would act in
324 the direction of elevating the (lower 25th percentile) assumed glacial concentrations above the glacial
325 atmospheric values and reducing the (upper 25th percentile) assumed interglacial concentrations. There is also
326 the potential for artificially elevated CO₂ concentrations in blue ice due in-situ respiration of CO₂ due to
327 microbial activity in detrital matter. Respiration effects are screened for by measurements of δ¹³C of CO₂,
328 however it is difficult to demonstrate that all samples are unaffected (Yan *et al.*, 2019). These uncertainties
329 support our argument that the GLS-model predictions are not rejected by the available observed BI-CO₂ data.

330

331 We consider the BI-CO₂ data to provide the most reliable measurements of CO₂ concentration, in the absence of
332 a continuous ice core record across the MPT. However, further comparison of our CO₂ predictions can also be
333 made against CO₂ proxy data from non-ice core archives (Fig 4A). We consider here δ¹¹B-based atmospheric
334 CO₂ reconstructions (Chalk *et al.*, 2017, Dyez *et al.* 2018 and Guillermic *et al.* 2022) and a recent atmospheric
335 CO₂ reconstruction from δ¹³C of leaf wax (Yamamoto *et al.*, 2022). The continuous δ¹¹B-based reconstructions
336 of Dyez *et al.*, (2018) overlap PRED-CO₂ from ~1.38 – 1.5 Mya while the Chalk *et al.*, (2017) reconstruction
337 overlaps PRED-CO₂ from 1.09 – 1.43 Mya. Discrete reconstructions from Guillermic *et al.* (2022) are
338 distributed non-uniformly across the ~800 to 1.5 Mya interval. For the two continuous δ¹¹B-based
339 reconstructions (Chalk *et al.*, (2017) and Dyez *et al.*, (2018)) the glacial CO₂ levels appear consistent with the
340 PRED-CO₂ record, within their reported 30 – 60 ppm uncertainties. However, δ¹¹B-based interglacial stages in
341 these reconstructions exceed those of the PRED-CO₂ record (Fig. 4A). The Guillermic *et al.* (2022)
342 reconstructions suggest a larger range of CO₂ concentrations than the overlapping intervals of PRED-CO₂ and of
343 the two continuous δ¹¹B-based reconstructions (Fig. 4A). The large range of the Guillermic *et al.* (2022) data
344 and the high interglacial maxima in the Chalk *et al.* (2017) and Dyez *et al.*, (2018) data, all significantly exceed
345 the range and interglacial maxima from the BI-CO₂ estimates. These discrepancies internally between different
346 δ¹¹B-based CO₂ reconstructions and between the δ¹¹B-based reconstructions and the BI-CO₂ data, may be due to
347 uncertainties associated with the δ¹¹B proxy transfer function. The δ¹¹B-based CO₂ reconstructions are
348 dependent on assumptions about multiple components of the carbonate system, including local marine carbon
349 chemistry and the CO₂ saturation state in the past (Hönisch *et al.*, 2009). Evidence that δ¹¹B-based

350 reconstructions may overestimate interglacial stage CO₂ is also seen in data from Chalk *et al.*, (2017) spanning
351 ca. 0–250 kya, where the δ¹¹B-based interglacial CO₂ levels exceed the continuous ice core CO₂ record by up to
352 ca. 30 ppm.

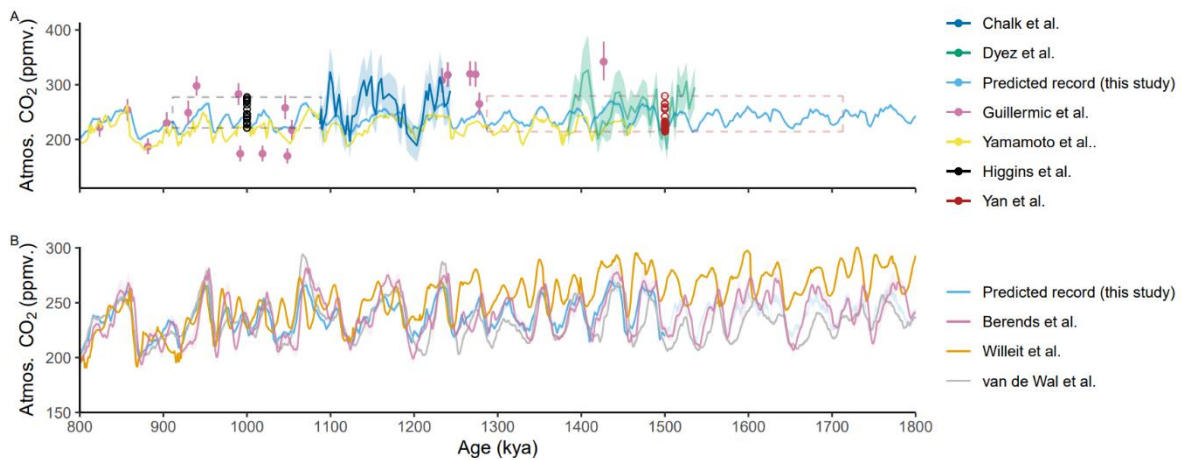
353

354 By comparison, the δ¹³C of leaf wax data (Yamamoto *et al.*, 2022) has a similar glacial to interglacial range as
355 PRED-CO₂, but a ca. 20ppm lower mean concentration than our predictions (Fig 4A). Hence, our PRED-CO₂
356 data fall lower than interglacial δ¹¹B-based interglacial levels but are higher than the δ¹³C of leaf-wax based
357 estimate. The strong spread between these different proxies and the large associated uncertainty of the
358 alternative marine and leaf wax proxy-CO₂ reconstructions mean that we do not find cause from the existing
359 CO₂ proxy data to reject our predictions nor our associated null-hypothesis.

360

361 We also compare our predictions to existing more complex model simulations (Fig 4B.). First, against a
362 transient simulation using an intermediate-complexity earth system model (CLIMBER-2) by Willeit *et al.*
363 (2019). This study suggests a combination of gradual regolith removal and atmospheric CO₂ decline can explain
364 the long-term climate variability over the past 3 Myr. Second, against a longer-term reconstruction by van de
365 Wal *et al.* (2011), which uses benthic δ¹⁸O that utilises deep-sea benthic isotope records to reconstruct a
366 continuous CO₂ record over the past 20 Myr. Third, a CO₂ reconstruction based on an inverse forward-
367 modelling approach forced by the LR04 benthic stack, in which the forward model is incrementally updated
368 through interaction with general circulation model snapshots and the ANICE 3-D ice-sheet-shelf model
369 (Berends *et al.* 2021b). Our simple GLS model demonstrates a similar long-term trend and timing of glacial-
370 interglacial signals and an atmospheric CO₂ level that sits approximately mid-way between the van de Wal *et al.*
371 (2011), and Willeit *et al.* (2019) models and is remarkably similar to the Berends *et al.* (2021b) reconstruction,
372 despite their different approach. Notably the Berends *et al.* reconstruction shows greater glacial to interglacial
373 amplitude in the CO₂ signal compared to our GLS-model. The decreasing linear trend in CO₂ in Willeit *et al.*
374 (2019), which is not seen in the other reconstructions, was directly prescribed in that study to induce Northern
375 Hemisphere glaciation at 2.6 Myr ago.

376



377

378 **Figure 4: A) Predicted CO₂ (this work) compared to observed, proxy CO₂ estimates from a range of other**
379 **sources: δ¹¹B-based pCO₂ reconstructions and measurements by Dyez *et al.* (2018), Guillermic *et al.***
380 **(2022); Chalk *et al.*, (2017); blue ice CO₂ measurements by Yan *et al.* (2019) and Higgins *et al.* (2015);**

381 **$\delta^{13}\text{C}$ leaf wax proxy reconstructions by Yamamoto *et al.* (2022). The dashed boxes indicate the dating**
382 **uncertainty and range of the respective BI-CO₂ records. B) Our predicted record compared to various**
383 **model simulations: a regolith removal hypothesis simulation by Willeit *et al.* (2019); and inverse-model**
384 **based CO₂ reconstructions by van de Wal *et al.* (2011), and Berends *et al.*, (2021b).**

385

386 A complete and critical test of our and other CO₂ predictions awaits the upcoming analysis of the continuous
387 oldest ice core records. We now discuss some potential applications of the PRED-CO₂ record for hypothesis
388 testing on the cause of the MPT.

389

390 PRED-CO₂ shows a long-term decline in glacial CO₂ across the MPT, but no long-term decrease in interglacial
391 CO₂. This pattern is consistent with the boron-isotope-based CO₂ reconstructions shown earlier, where it is often
392 described as an increase in the interglacial to glacial CO₂ difference (e.g., Chalk *et al.*, 2017; Hönisch *et al.*,
393 2009). Chalk *et al.*, (2017) concludes that the MPT was initiated by a change in ice sheet dynamics and that
394 longer and higher-ice volume post-MPT ice ages are sustained by carbon cycle feedbacks, in particular dust
395 fertilisation of the Southern Ocean. The fact that our LR04-based prediction of CO₂ captures this same trend,
396 with predicted glacial CO₂ fairly constant from 1.5 to ca. 1.0 Mya before declining from 1.0 to 0.6 Mya, reflects
397 that the LR04 benthic stack also features an increase in the interglacial to glacial benthic $\delta^{18}\text{O}$ difference across
398 this same interval, which is dominated by the glacial stage changes (Fig 3A.). Here, a comparison of PRED-CO₂
399 to a realised continuous oldest ice core record will be of value. The agreement or disagreement would inform on
400 the proportionality of the CO₂ coupling with ice volume; if there were a major new or non-linear process across
401 the MPT that changed the nature of coupling between CO₂ and ice volume the PRED-CO₂ and observed CO₂
402 records would be expected to diverge.

403

404 Another avenue to use the PRED-CO₂ record for hypothesis testing on the cause of the MPT concerns the phase
405 locking hypothesis. The phase locking hypothesis is proposed to explain the absence of precession-related (23
406 kyr) periods in the LR04 benthic stack prior to the MPT (Fig 1), despite the strong precession cycle in insolation
407 (Raymo *et al.*, 2006, Morée *et al.*, 2021). The key concept is that prior to the MPT the Northern Hemisphere and
408 Antarctic ice sheets were responsive (in ice volume) to insolation changes in the precession band, but because
409 precession forcing is out of phase between the hemispheres, the ice volume changes were opposing between the
410 hemispheres and therefore cancelled in the benthic stack. This cancellation of the precession signal left
411 insolation forcing in the 41 kyr obliquity band to dominate globally integrated ice volume changes expressed in
412 the benthic stack. A transition from a smaller and more dynamic terrestrial-terminating Antarctic ice sheet to a
413 larger and more stable marine-terminating ice sheet with cooling climate across the MPT (e.g. Elderfield *et al.*,
414 2012) is then proposed to remove sensitivity of Antarctic ice volume to local precession forcing in favour of
415 quasi-100 kyr ice volume changes that are in phase between the hemispheres (Raymo *et al.*, 2006).

416

417 Recently presented data from Yan *et al.* (2022), lend some support to the phase locking hypothesis, specifically
418 with evidence that pre-MPT Antarctic temperature (and by extension ice volume) is positively correlated with a
419 local precession-band insolation proxy based on the oxygen to nitrogen ratio of trapped air (Yan *et al.*, 2022).
420 Whereas the correlation becomes negative in the blue ice and continuous ice core data in the post-MPT record.

421 If Yan *et al.*, (2022) is correct and the phase locking hypothesis holds, then an implication is that prior to the
422 MPT, Antarctic climate, Antarctic ice volume and by extension Southern Ocean climate conditions, would fall
423 out of phase with the LR04 benthic stack. To now extend the argument to potential impacts on CO₂ exchange, if
424 the phase locking hypothesis holds, then prior to the MPT the Antarctic and Southern Ocean climate conditions
425 and by extension the Southern Ocean mechanisms of CO₂ exchange described earlier, would also be expected to
426 fall out of phase with the benthic stack. Since our regression model assumes continuation of the in-phase
427 relationship between the benthic stack and Antarctic and Southern Ocean climate conditions (as inherited from
428 the post-MPT training data) we would expect to see major disagreement between our pre-MPT CO₂ predictions
429 and a realised oldest ice continuous ice core CO₂ record.

430

431 **5 Summary and Conclusions**

432 In this study we have used a simple generalised least squares (GLS) model to predict atmospheric CO₂ from the
433 LR04 benthic $\delta^{18}\text{O}$ stack for the period spanning the mid-Pleistocene transition, 800–1800 kyr. Our CO₂
434 prediction is therefore based on the assumption that the physical processes linking CO₂, sea level, global ice
435 volume and ocean temperature over the past 800 kyr do not fundamentally change across the 800–1800 kya time
436 period. The null-hypothesis is deliberately simplistic on the basis that differences between our predictions and
437 observed or proxy CO₂ records may be revealing of the physical processes involved in the mid-Pleistocene
438 Transition.

439

440 We made initial tests of the null hypothesis by comparing our predicted CO₂ record to existing discrete blue ice
441 CO₂ records and other non-ice-core proxy-CO₂ records from the 800–1800 kyr interval. Our predicted CO₂
442 concentrations do not show any systematic departure from observed blue ice CO₂ concentrations. The
443 predictions are marginally lower (during glacial *and* interglacial stages) than those observed in blue ice from
444 1000 ± 89 kya and marginally higher than observed in blue ice data from $1.5 \text{ Mya} \pm 213$ kyr. Our predictions
445 were generally lower than interglacial $\delta^{11}\text{B}$ -based-CO₂ reconstructions, but higher than recent $\delta^{13}\text{C}$ of leaf-wax
446 based CO₂ reconstructions. Overall, we do not find clear evidence from the existing blue ice or proxy CO₂ data
447 to reject our predictions nor our associated null-hypothesis. The definitive test of our and other CO₂ predictions
448 therefore awaits the future analysis of the upcoming continuous oldest ice core records. The PRED-CO₂ record
449 presented here should provide a useful comparison to forthcoming oldest ice core records and opportunity to
450 provide further constraints on the processes involved in the MPT.

451

452 **Author contributions**

453 Project design by JBP, TRV and JRWM and supervision by TRV and JBP. Data analysis and figures by JRWM
454 with input from all authors. Writing led by JRMV and JBP. All authors contributed to and agreed on the final
455 version of the manuscript.

456

457 **Competing interests**

458 The authors declare that they have no competing interests.

459

460 **Disclaimer**

461 This study, to the best of the author(s) knowledge and belief, contains no material previously published or
462 written by another person, except where due reference is made in the text of the study.

463

464 **Acknowledgements**

465 We acknowledge assistance from Simon Wotherspoon (Institute for Marine and Antarctic Studies) in
466 appropriate model selection methods. We thank Lorraine Lisiecki and Constantijn Berends's for their
467 constructive reviews, which greatly improved the manuscript. This research was supported by the Australian
468 Government through Australian Antarctic Science projects 4632, the Million Year Ice Core (MYIC) Project and
469 by the Australian Government Department of Industry Science Energy and Resources, grant ASCI000002.

470

471 **Data availability**

472 The PRED-CO₂ data presented here will be publicly archived at the Australian Antarctic Data Centre
473 (https://data.aad.gov.au/metadata/AAS_4632_Martin_et_al_CP_2024

474

475 **References**

- 476 Archer, D., Winguth, A., D. Lea, and Mahowald, N.: What caused the glacial/interglacial atmospheric
477 pCO₂ cycle?, *Rev. Geophys.*, 38, 159–189, 2000, <https://doi.org/10.1029/1999RG000066>, 2000.
- 478
- 479 Bazin, L., Landais, A., Lemieux-Dudon, B., Toye Mahamadou Kele, H., Veres, D., Parrenin, F., Martinerie, P.,
480 Ritz, C., Capron, E., Lipenkov, V., Loutre, M.-F., Raynaud, D., Vinther, B., Svensson, A., Rasmussen, S.,
481 Severi, M., Blunier, T., Leuenberger, M., Fischer, H., Masson-Delmotte, V., Chappellaz, J., and Wolff, E.: An
482 optimized multi-proxies, multi-site Antarctic ice and gas orbital chronology (AICC2012): 120-800 ka, *Clim.*
483 *Past*, 9, 1715-1731, <https://doi.org/10.5194/cp-9-1715-2013>, 2013.
- 484
- 485 Bereiter, B., Eggleston, S., Schmitt, J., Nehrbass-Ahles, C., Stocker, T. F., Fischer, H., Kipfstuhl, S., and
486 Chappellaz, J.: Revision of the EPICA Dome C CO₂ record from 800 to 600 ky before present, *Geophys. Res.*
487 *Lett.*, 42, 542-549, <https://doi.org/10.1002/2014gl061957>, 2015.
- 488
- 489 Berends, C. J., Köhler, P., Lourens, L. J., and van de Wal, R. S. W.: On the cause of the mid-Pleistocene
490 transition., *Rev. Geophys.*, 59, e2020RG000727. <https://doi.org/10.1029/2020RG000727>, 2021a.
- 491
- 492 Berends, C. J., de Boer, B., and van de Wal, R. S. W.: Reconstructing the evolution of ice sheets, sea level, and
493 atmospheric CO₂ during the past 3.6 million years. *Clim. Past*, 17, 361–377, [http://doi.org/10.5194/cp-17-361-](http://doi.org/10.5194/cp-17-361-2021)
494 [2021](http://doi.org/10.5194/cp-17-361-2021), 2021b.
- 495
- 496 Berger, A., Li, X. S., and Loutre, M. F.: Modelling northern hemisphere ice volume over the last 3Ma,
497 *Quaternary. Sci. Rev.*, 18, 1-11, [https://doi.org/10.1016/S0277-3791\(98\)00033-X](https://doi.org/10.1016/S0277-3791(98)00033-X), 1999.
- 498
- 499 Broecker, W.S.: Glacial to interglacial changes in ocean chemistry, *Prog. Oceanogr.*, 11 (2), 151-197.
500 [https://doi.org/10.1016/0079-6611\(82\)90007-6](https://doi.org/10.1016/0079-6611(82)90007-6), 1982.
- 501
- 502 Chalk, T., Hain, M., Foster, G., Rohling, E., Sexton, P., Badger, M., Cherry, S., Hasenfratz, A., Haug, G.,
503 Jaccard, S., Martínez-García, A., Pälike, H., Pancost, R., and Wilson, P.: Causes of ice age intensification across
504 the Mid-Pleistocene Transition, *P. Natl. Acad. Sci. USA.*, 114, 13114-13119,
505 <https://doi.org/10.1073/pnas.1702143114>, 2017.
- 506
- 507 Clark, P. U., Archer, D., Pollard, D., Blum, J. D., Rial, J. A., Brovkin, V., Mix, A. C., Pisias, N. G., and Roy,
508 M.: The middle Pleistocene transition: characteristics, mechanisms, and implications for long-term changes in
509 atmospheric pCO₂, *Quat. Sci. Rev.*, 25, 3150-3184, <https://doi.org/10.1016/j.quascirev.2006.07.008>, 2006.
- 510
- 511 Clark, P. U. and Pollard, D.: Origin of the Middle Pleistocene Transition by ice sheet erosion of regolith,
512 *Paleoceanography*, 13, 1-9, <https://doi.org/10.1029/97pa02660>, 1998.

513
514 Dyez, K.A., Hönisch, B., and Schmidt, G.A.: Early Pleistocene obliquity-scale pCO₂ variability at ~1.5 million
515 years ago. *Paleoceanogr. Paleoclimatol.*, 33, no. 11, 1270-1291, <https://doi.org/10.1029/2018PA003349>, 2018.
516
517 Elderfield, H., Ferretti, P., Greaves, S., Crowhurst, S., McCave, N., and Piotrowski, A.M.: Evolution of Ocean
518 Temperature and Ice Volume Through the Mid-Pleistocene Climate Transition, *Science*, 337,704-709,
519 <https://doi.org/10.1126/science.1221294>, 2012.
520
521 Gottschalk, J., Battaglia, G., Fischer, H., Frölicher, T.L., Jaccard, S.L., Jeltsch-Thömmes, A., Joos, F., Köhler,
522 P., Meissner, K.J., Menviel, L., Nehrbass-Ahles, C., Schmitt, J., Schmittner, A., Skinner, L.C., and Stocker,
523 T.G.: Mechanisms of millennial-scale atmospheric CO₂ change in numerical model simulations, *Quaternary*.
524 *Sci. Rev.*, 220, 30-74, <https://doi.org/10.1016/j.quascirev.2019.05.013>, 2019.
525
526 Guillermic, M., Misra, S., Eagle, R., and Tripathi, A.: Atmospheric CO₂ estimates for the Miocene to Pleistocene
527 based on foraminiferal δ¹¹B at Ocean Drilling Program Sites 806 and 807 in the Western Equatorial Pacific,
528 *Clim. Past*, 18(2), 183-207, <https://doi.org/10.5194/cp-18-183-2022>, 2022.
529
530 Hasenfratz, A. P., Jaccard, S. L., Martínez-García, A., Sigman, D. M., Hodell, D. A., Vance, D., Bernasconi, S.
531 M., Kleiven, H. F., Haumann, F. A., and Haug, G. H.: The residence time of Southern Ocean surface waters and
532 the 100,000-year ice age cycle, *Science*, 363, 1080, <https://doi.org/10.1126/science.aat7067>, 2019.
533
534 Higgins, J. A., Kurbatov, A. V., Spaulding, N. E., Brook, E., Introne, D. S., Chimiak, L. M., Yan, Y.,
535 Mayewski, P. A., and Bender, M. L.: Atmospheric composition 1 million years ago from blue ice in the Allan
536 Hills, Antarctica, *P. Natl. Acad. Sci. USA.*, 112, 6887, <https://doi.org/10.1073/pnas.1420232112>, 2015.
537
538 Hönisch, B., Hemming, N. G., Archer, D., Siddall, M., and McManus, J. F.: Atmospheric Carbon Dioxide
539 Concentration Across the Mid-Pleistocene Transition, *Science*, 324, 1551,
540 <https://doi.org/10.1126/science.1171477>, 2009.
541
542 Huybers, P., & Wunsch, C. (2005). Obliquity pacing of the late Pleistocene glacial terminations. *Nature*,
543 434(7032), 491-494.
544
545 International Panel on Climate Change: Climate change 2001; IPCC third assessment report, IPCC, Geneva,
546 2001.
547
548 International Partnerships in Ice Core Sciences: The oldest ice core: A 1.5 million year record of climate and
549 greenhouse gases from Antarctica [White paper]. [https://igbp-](https://igbp-scor.pages.unibe.ch/sites/default/files/download/docs/working_groups/ipics/white-papers/ipics_oldda_final.pdf)
550 [scor.pages.unibe.ch/sites/default/files/download/docs/working_groups/ipics/white-papers/ipics_oldda_final.pdf](https://igbp-scor.pages.unibe.ch/sites/default/files/download/docs/working_groups/ipics/white-papers/ipics_oldda_final.pdf),
551 accessed 06/12/2023, 2020.
552
553 Jouzel, J., Masson-Delmotte, V., Cattani, O., Dreyfus, G., Falourd, S., Hoffmann, G., Minster, B., Nouet, J.,
554 Barnola, J. M., Chappellaz, J., Fischer, H., Gallet, J. C., Johnsen, S., Leuenberger, M., Loulergue, L., Luethi, D.,
555 Oerter, H., Parrenin, F., Raisbeck, G., Raynaud, D., Schilt, A., Schwander, J., Selmo, E., Souchez, R., Spahni,
556 R., Stauffer, B., Steffensen, J. P., Stenni, B., Stocker, T. F., Tison, J. L., Werner, M., and Wolff, E. W.: Orbital
557 and Millennial Antarctic Climate Variability over the Past 800,000 Years, *Science*, 317, 793,
558 <https://doi.org/10.1126/science.1141038>, 2007.
559
560 Lisiecki, L. E. and Raymo, M. E.: A Pliocene-Pleistocene stack of 57 globally distributed benthic δ¹⁸O records,
561 *Paleoceanography*, 20, PA1003, <https://doi.org/10.1029/2004pa001071>, 2005.
562
563 Martínez-García, A., Sigman, D.M., Ren, H., Anderson, R.F., Straub, M., Hodell, D.A., Jaccard, S.L., Eglinton,
564 T.I., and Haug, G.H.: Iron fertilization of the subantarctic ocean during the last ice age, *Science*, 343 (6177),
565 1347-1350, <https://doi.org/10.1126/science.1246848>, 2014.
566
567 McClymont, E.L., Sosdian, S.M., and Rosell-Melé, A.: Pleistocene sea-surface temperature evolution: Early
568 cooling, delayed glacial intensification, and implications for the mid-Pleistocene transition. *Earth. Sci. Rev.*,
569 123, 173-193, <https://doi.org/10.1016/j.earscirev.2013.04.006>, 2013.
570
571 Millero, F. J.: Thermodynamics of the carbon dioxide system in the oceans, *Geochim. Cosmochim. Acta.*, 59,
572 661-677, [https://doi.org/10.1016/0016-7037\(94\)00354-O](https://doi.org/10.1016/0016-7037(94)00354-O), 1995.

573
574 Morée, A. L., Sun, T., Bretones, A., Straume, E. O., Nisancioglu, K., and Gebbie, G.: Cancellation of the
575 precessional cycle in $\delta^{18}\text{O}$ records during the Early Pleistocene. *Geophys. Res. Lett.*, 48,
576 e2020GL090035. <https://doi.org/10.1029/2020GL090035>, 2021.

577
578 Petit, J. R., Jouzel, J., Raynaud, D., Barkov, N. I., Barnola, J. M., Basile, I., Bender, M., Chappellaz, J., Davis,
579 M., Delaygue, G., Delmotte, M., Kotlyakov, V. M., Legrand, M., Lipenkov, V. Y., Lorius, C., Pépin, L., Ritz,
580 C., Saltzman, E., and Stievenard, M.: Climate and atmospheric history of the past 420,000 years from the
581 Vostok ice core, Antarctica, *Nature*, 399, 429-436, <https://doi.org/10.1038/20859>, 1999.

582
583 Raymo, M., Lisiecki, L., and Nisancioglu, K.: Plio-Pleistocene Ice Volume, Antarctic Climate, and the Global
584 18O Record, *Science*, 313, 492-495, <https://doi.org/10.1126/science.1123296>, 2006.

585
586 Raymo, M., Ruddiman, W., and Froelich, P.: Influence of Late Cenozoic mountain building on ocean
587 geochemical cycles, *Geology*, 16, 649-653, [https://doi.org/10.1130/0091-](https://doi.org/10.1130/0091-7613(1988)016<0649:IOLCMB>2.3.CO;2)
588 [7613\(1988\)016<0649:IOLCMB>2.3.CO;2](https://doi.org/10.1130/0091-7613(1988)016<0649:IOLCMB>2.3.CO;2), 1988.

589
590 Raymo, M. E.: The timing of major climate terminations, *Paleoceanography*, 12, 577-585,
591 <https://doi.org/10.1029/97PA01169>, 1997.

592
593
594 Röthlisberger, R., Bigler, M., Wolff, E. W., Joos, F., Monnin, E., and Hutterli, M. A.: Ice core evidence for the
595 extent of past atmospheric CO_2 change due to iron fertilisation, *Geophys. Res. Lett.*, 31, L16207,
596 <https://doi.org/10.1029/2004GL020338>, 2004.

597
598 Ruddiman, W. F., Raymo, M. E., Martinson, D. G., Clement, B. M., and Backman, J.: Pleistocene evolution:
599 Northern hemisphere ice sheets and North Atlantic Ocean, *Paleoceanography*, 4, 353-412,
600 <https://doi.org/10.1029/PA004i004p00353>, 1989.

601
602 Shackleton, N. J. and Pisias, N. G.: Atmospheric Carbon Dioxide, Orbital Forcing, and Climate. In: *The Carbon*
603 *Cycle and Atmospheric CO_2 : Natural Variations Archean to Present*, <https://doi.org/10.1029/GM032p0303>,
604 1985.

605
606 Shugi, H., The older the ice, the better the science. *Adv. Polar Sci.*, 23, 121-122,
607 <https://doi.org/10.13679/j.advps.2022.0004>, 2022.

608
609 Stephens, B.B., Keeling, R.F.: The influence of Antarctic sea ice on glacial–interglacial CO_2 variations. *Nature*,
610 404, 171–174, <https://doi.org/10.1038/35004556>, 2000.

611
612 Tzedakis, P. C., Crucifix, M., Mitsui, T., and Wolff, E. W.: A simple rule to determine which insolation cycles
613 lead to interglacials, *Nature*, 542, 427-432, <https://doi.org/10.1038/nature21364>, 2017.

614
615 Ushie, H., and Matsumoto, K.: The role of shelf nutrients on glacial-interglacial CO_2 : A negative
616 feedback, *Global Biogeochem. Cy.*, 26, GB2039, <https://doi.org/10.1029/2011GB004147>., 2012.

617
618 van de Wal, R. S. W., de Boer, B., Lourens, L. J., Köhler, P., and Bintanja, R.: Reconstruction of a continuous
619 high-resolution CO_2 record over the past 20 million years. *Clim. Past*, 7, 1459–1469. [https://doi.org/10.5194/cp-](https://doi.org/10.5194/cp-7-1459-2011)
620 [7-1459-2011](https://doi.org/10.5194/cp-7-1459-2011), 2011.

621
622 Veres, D., Bazin, L., Landais, A., Toyé Mahamadou Kele, H., Lemieux-Dudon, B., Parrenin, F., Martinerie, P.,
623 Blayo, E., Blunier, T., Capron, E., Chappellaz, J., Rasmussen, S., Severi, M., Svensson, A., Vinther, B., and
624 Wolff, E.: The Antarctic ice core chronology (AICC2012): an optimized multi-parameter and multi-site dating
625 approach for the last 120 thousand years, *Clim. Past*, 9, 1733-1748, <https://doi.org/10.5194/cp-9-1733-2013>,
626 2013.

627
628 Willeit, M., Ganopolski, A., Calov, R., and Brovkin, V.: Mid-Pleistocene transition in glacial cycles explained by
629 declining CO_2 and regolith removal, *Sci. Adv.*, 5, eaav7337, doi: 10.1126/sciadv.aav7337, 2019.

630

631 Wolff, E. W., Chappella, J., Fischer, H., Kull, C., Miller, H., Stocker, T. F., and Watson, A. J.: The EPICA
632 challenge to the Earth system modeling community, *EOS*, 85, 363363, <https://doi.org/10.1029/2004EO380003>,
633 2004.
634
635 Wolff, E. W., Kull, C., Chappellaz, J., Fischer, H., Miller, H., Stocker, T. F., Watson, A. J., Flower, B., Joos, F.,
636 Köhler, P., Matsumoto, K., Monnin, E., Mudelsee, M., Paillard, D., and Shackleton, N.: Modeling past
637 atmospheric CO₂: results of a challenge, *EOS*, 86 (38), 341-345, <http://doi.org/10.1029/2005EO380003>, 2005.
638
639 Yamamoto, M., Clemens, S.C., Seki, O., Tsuchiya, Y., Huang, Y., O'ishi, R., and Abe-Ouchi, A.: Increased
640 interglacial atmospheric CO₂ levels followed the mid-Pleistocene Transition, *Nat. Geosci.*, 15(4), 307–313,
641 <https://doi.org/10.1038/s41561-022-00918-1>, 2022.
642
643 Yan, Y., Bender, M.L., Brook, E.J., Clifford, H.M., Kemény, P.C., Kurbatov, A.V., Mackay, S., Mayewski,
644 P.A., Ng, J., Severinghaus, J.P., and Higgins, J.A.: Two-million-year-old snapshots of atmospheric gases from
645 Antarctic ice, *Nature*, 574(7780), 663–666, <https://doi.org/10.1038/s41586-019-1692-3>, 2019.
646
647 Yan, Y., Kurbatov, A.V., Mayewski, P.A., Shackleton, S., and Higgins, J.A.: Early Pleistocene East Antarctic
648 temperature in phase with local insolation. *Nat. Geosci.*, 16, 50-55, [https://doi.org/10.1038/s41561-022-01095-](https://doi.org/10.1038/s41561-022-01095-x)
649 x, 2022.